

HSL-knockout mouse testis exhibits class B scavenger receptor upregulation and disrupted lipid raft microdomains^S

María Emilia Casado,^{*,§} Lydia Huerta,^{*} Ana Isabel Ortiz,[†] Mirian Pérez-Crespo,^{**} Alfonso Gutiérrez-Adán,^{**} Fredric B. Kraemer,^{††} Miguel Ángel Lasunción,^{*,§,§§} Rebeca Busto,^{1,*,§} and Antonia Martín-Hidalgo^{1,2,*,§}

Servicio de Bioquímica-Investigación* and Unidad de Cirugía Experimental y Animalario,[†] Hospital Universitario Ramón y Cajal, Instituto Ramón y Cajal de Investigación Sanitaria (IRYCIS), Madrid, Spain; CIBER de Fisiopatología de la Obesidad y Nutrición (CIBERObn),[§] Instituto de Salud Carlos III (ISCIII), Spain; Dpto. de Reproducción Animal y Conservación de Recursos Zoogenéticos,^{**} Instituto Nacional de Investigación y Tecnología Agraria y Alimentaria (INIA), Madrid, Spain; Stanford University and VA Palo Alto Health Care System,^{††} Palo Alto, CA; and Departamento de Bioquímica y Biología Molecular,^{§§} Universidad de Alcalá, Madrid, Spain

Abstract There is a tight relationship between fertility and changes in cholesterol metabolism during spermatogenesis. In the testis, class B scavenger receptors (SR-B) SR-BI, SR-BII, and LIMP II mediate the selective uptake of cholesterol esters from HDL, which are hydrolyzed to unesterified cholesterol by hormone-sensitive lipase (HSL). HSL is critical because HSL knockout (KO) male mice are sterile. The aim of the present work was to determine the effects of the lack of HSL in testis on the expression of SR-B, lipid raft composition, and related cell signaling pathways. HSL-KO mouse testis presented altered spermatogenesis associated with decreased sperm counts, sperm motility, and infertility. In wild-type (WT) testis, HSL is expressed in elongated spermatids; SR-BI, in Leydig cells and spermatids; SR-BII, in spermatocytes and spermatids but not in Leydig cells; and LIMP II, in Sertoli and Leydig cells. HSL knockout male mice have increased expression of class B scavenger receptors, disrupted caveolin-1 localization in lipid raft plasma membrane microdomains, and activated phospho-ERK, phospho-AKT, and phospho-SRC in the testis, suggesting that class B scavenger receptors are involved in cholesterol ester uptake for steroidogenesis and spermatogenesis in the testis.—Casado, M. E., L. Huerta, A. I. Ortiz, M. Pérez-Crespo, A. Gutiérrez-Adán, F. B. Kraemer, M. Á. Lasunción, R. Busto, and A. Martín-Hidalgo. **HSL-knockout mouse testis exhibits class B scavenger receptor upregulation and disrupted lipid raft microdomains.** *J. Lipid Res.* 2012. 53: 2586–2597.

Supplementary key words hormone-sensitive lipase • cholesterol esters • steroidogenesis • spermatogenesis • fertility • sterility

Spermatogenesis occurs in a series of proliferative and differentiation stages, which can be subdivided into mitotic, meiotic, and spermatogenic phases. Each phase is characterized by distinct cell types (spermatogonia, spermatocytes, and spermatids, respectively) (1, 2). Pathologic, experimental, and natural seasonal arrest of spermatogenesis are all associated with increases in lipid droplets (3, 4), indicating a close relationship between fertility and changes in lipid metabolism during spermatogenesis (5). A constant supply of cholesterol is required within Leydig cells to serve as precursor for the synthesis of steroid hormones (steroidogenesis) (6, 7), whereas in the seminiferous tubules, cholesterol is involved in germinal cell differentiation to spermatozooids (spermatogenesis or gametogenesis) (8). There is also considerable evidence indicating that cholesterol is required for the development of gametes and fertility in both sexes. Disruption of the DHCR24 gene, which encodes the cholesterol biosynthetic enzyme desmosterol reductase, causes infertility in male mice (9). In addition to cholesterol, sterol

Abbreviations: Cav-1, caveolin-1; CE, cholesteryl ester; CEH, cholesteryl ester hydrolase; DAG, diacylglycerol; FF-MAS, follicular fluid meiosis-activating sterol; HSL, hormone-sensitive lipase; KO, knockout; LC, Leydig cell; MAG, monoacylglycerol; MC, myoid cell; PI3K, phosphoinositide-3-kinase; RE, retinyl ester; rS, round spermatid; S, Sertoli; Sc, spermatocyte; Sp, elongated spermatid; SR-B, class B scavenger receptor; ST, seminiferous tubule; StAR, steroidogenic acute regulatory; TAG, triacylglycerol; TfR, transferrin receptor; T-MAS, testicular meiosis-activating sterol; WT, wild-type.

¹R. Busto and A. Martín-Hidalgo contributed equally to this work.

²To whom correspondence should be addressed.

e-mail: antonia.martin@hrc.es

^SThe online version of this article (available at <http://www.jlr.org>) contains supplementary data in the form of one table and one figure.

This work was supported by grants from the Ministerio de Ciencia e Innovación (SAF2009-08764 and SAF2011-29951) and Fondo de Investigación Sanitaria (PI081063), Spain, and by the Department of Veterans Affairs (Office of Research and Development, Medical Research Service). CIBER de la Fisiopatología de la Obesidad y Nutrición is an initiative of ISCIII. R.B. is an investigator for FIBio-HRC, supported by Comunidad de Madrid and the Fondo de Investigación Sanitaria.

Manuscript received 8 May 2012 and in revised form 13 September 2012.

Published, JLR Papers in Press, September 17, 2012

DOI 10.1194/jlr.M028076

intermediates in the cholesterol biosynthesis pathway, such as follicular fluid meiosis activating sterol (FF-MAS) and testicular meiosis activating sterol (T-MAS), are biologically active as stimulators of meiosis in the gonads (10).

Considerable amounts of cholesterol are present inside seminiferous tubules (11). The cholesterol used for steroidogenesis or spermatogenesis is derived from different sources (6), as follows: de novo cholesterol synthesis; mobilization of stored cholesterol esters (CE) via the action of neutral cholesteryl ester hydrolase activities (CEH or hormone-sensitive lipase [HSL]); lipoprotein-derived cholesterol via the LDL receptor-mediated endocytic pathway; and class B scavenger receptor (SR-B) (SR-BI, SR-BII, and LIMP II)-mediated "selective" HDL cholesteryl ester uptake pathway. Sertoli cells possess the capacity to synthesize cholesterol from acetate *in vitro* (12), but it seems unlikely that this source is sufficient to sustain steroidogenesis *in vivo*. Actually, at least in rodents, it appears that HDL is the major source of cholesterol for Sertoli cells (13).

A striking correlation has been demonstrated between the enhanced lipid uptake from HDL, promoted by the induction of SR-BI expression and steroid biosynthesis in steroidogenic cells (14–16). The vast majority of lipoprotein-derived cholesterol utilized for murine steroidogenesis in testes is obtained via SR-B (7). The SR-B are multiligand membrane proteins highly expressed in tissues with a strong cholesterol demand for steroidogenesis, such as the adrenals, ovaries, and testes (14, 17). SR-B are responsible of the "selective uptake of cholesteryl esters" from HDL by steroidogenic cells (18–20). In the testis, SR-BI is most abundantly expressed in steroidogenic Leydig cells (7, 14), with lesser amounts in Sertoli cells (21). Experimental deficiency of SR-BI causes abnormalities in the development of female gametes. A significant proportion of ovulated oocytes die soon after ovulation, all resulting in sterility in SR-BI gene-knockout (KO) female mice (22).

HSL is an intracellular neutral lipase that hydrolyzes triacylglycerols (TAG), diacylglycerols (DAG), monoacylglycerols (MAG), CE, and retinyl esters (RE) (23). In fact, the relative maximal hydrolysis rates are in the range of 1:10:1:4:2 for TAG, DAG, MAG, CE, and RE, respectively. These data suggest that HSL has more DAG and CE hydrolase activities than TAG hydrolase activity. HSL is expressed in white and brown adipose tissues, and in several nonadipose tissues, including placenta, macrophages, heart, skeletal muscle, mammary glands, pancreatic β -cells, adrenal glands, ovaries, and testes (24–29). This multifunctional enzyme has emerged as a key regulator of cholesterol metabolism in steroidogenic tissues (adrenals, ovaries, and testes) (30) as responsible for the hydrolysis of intracellular CE, including those coming from CE selective uptake mediated by SR-B receptors (30). The direct interaction of HSL with steroidogenic acute regulatory protein (StAR) in cytosol increases the hydrolytic activity of HSL and facilitates cholesterol movement from stored lipid droplets to mitochondria for steroidogenesis (30, 31).

The testis expresses several protein species of HSL with apparent molecular masses ranging from 26 to 130 kDa, which are encoded by a single 3.9 kb HSL mRNA in rat

testis (26) and both 3.3 kb and 3.9 kb HSL mRNAs in human testis (27, 32). HSL is localized to elongated spermatids and Sertoli cells guinea pig and mink testis (8, 33). In the rat, HSL is only located in the seminiferous tubules (Sertoli and spermatogenic cells) (34), whereas in the normal human testis, HSL is detected in seminiferous tubules and Leydig cells (35).

The role of HSL in testis was revealed by the phenotype of HSL-deficient mice (4, 36). Male mice homozygous for the mutant allele (HSL^{-/-}) are sterile and show abnormalities in spermatogenesis, resulting in profound alterations in spermatid maturation and oligospermia (4). Because HSL catalyzes the hydrolysis of CE, it is reasonable to speculate that cholesterol released by the action of HSL is required for spermatogenesis. The lack of HSL is accompanied by a 2- to 4-fold increase in the accumulation of CE in the testis (4, 36) and decreased testis weights (4). The expression of the testicular form of HSL (HSLtes) in postmeiotic germ cells rescues the male infertility observed in HSL-deficient mice (37). These results and the presence of HSL in spermatids (4, 35) revealed the rate-limiting role of HSLtes and the importance of CEH activity in the action of HSL on spermatogenesis and, more specifically, on spermiogenesis.

In membranes, cholesterol is concentrated in lipid rafts, which are also enriched in sphingolipids (38). Lipid rafts serve as major platforms for the initiation, propagation, and maintenance of signal transduction events (39). Thus, it is not surprising that dysfunction in cholesterol synthesis, storage, transport, and removal in mice testis may lead to infertility. Many key signaling molecules have been shown to function via lipid rafts; examples of such molecules are SR-BI and SR-BII. Several authors reported that these receptors localize to cholesterol-rich plasma membrane caveolae (40, 41), which influence cholesterol homeostasis by acting as conduits for cellular flux (38) and which concentrate signaling proteins for signal transduction (39). In this regard, the MAPK signaling pathway has been shown to be activated when SR-BI is bound by its ligand (42, 43). However, in different cell types, Peng et al. (44) showed that SR-BI is localized primarily in clusters on microvillar extensions of the plasma membrane, whereas it is nearly absent from caveolae.

The main objective of the present work was to study the changes in the expression of SR-B (SR-BI, SR-BII, and LIMP II), as well as their association with lipid rafts and relevant signaling pathways in HSL^{-/-} mouse testis, to gain insight on the mechanisms mediating the alterations in spermatogenesis and, ultimately, infertility in these animals.

MATERIALS AND METHODS

Mice and tissue collection

Wild-type (WT) or (HSL^{+/+}) and HSL knockout (KO) or (HSL^{-/-}) mice from our colony weighing 25–30 g (approximately 4 months old) were used in this study. Mice were maintained at 22–24°C under standard conditions of illumination (08:00–20:00 h) and feeding (Purina Chow diet; Panlab, Barcelona, Spain). The animals

were fed ad libitum and had continuous access to tap water. The experimental protocol was approved by the Animal Research Ethics Committee (CEBA) of the Hospital Universitario Ramón y Cajal (Madrid, Spain).

The generation of mice with a targeted disruption of the Lipe gene encoding HSL ($HSL^{-/-}$) has been reported; these mice have no detectable HSL activity or protein in any tissue, including the testis (4, 36). $HSL^{\beta}/F1$ mice were bred for more than 5 generations into a C57BL/6 background. Given that homozygote males are infertile, to maintain the transgenic mice colony, heterozygote females were mated with heterozygote males. The pups were maintained with the mothers until the end of the lactating phase. Two weeks after weaning, males and females were separated in individual cages. Mice were genotyped by PCR analysis of tail DNA, as described previously (4).

At least seven mice from each experimental group were analyzed when 4 months old. Mice had free access to food and were euthanized by cervical dislocation between 10:00 and 11:00 h. Whole-animal body and testicular weights were recorded. Mouse testes were removed, one of which was frozen in liquid nitrogen and stored at -80°C until processing, and another testis was fixed in 4% paraformaldehyde for 6–24 h at 4°C . The fixed tissues were embedded in paraffin following conventional methods (28) and sectioned at $5\ \mu\text{m}$, either to be stained with hematoxylin and eosin or to be used for immunohistochemistry.

Plasma testosterone, total cholesterol, and triglycerides

Plasma testosterone was measured by ELISA with the kit from Cayman Chemical. Total cholesterol and TAG were measured by using the kits Cholesterol-Liquids CHO-PAD and GPO-PAP liquid, respectively, from Bradford Diagnostics (Kemia Científica).

Mice sperm collection for spermatozoa counts and motility

After animals were euthanized, cauda epididymis and vasa deferentia were retrieved and placed in M2 medium (Sigma Aldrich) after removing all excess adipose tissue and blood vessels to minimize the risk of contamination (45). Spermatozoa were released from the epididymis by slicing with a 30 gauge needle and left in the medium for 5 min to recover motility.

Determination of sperm characteristics

For the determination of sperm concentration, a Bürker hemocytometer was used. The number of spermatozoa was counted under a light microscope. For determination of motile sperm, semen was loaded into a prewarmed (37°C) slide and placed on the heated (37°C) microscope stage, and the percentages of motile spermatozoa were assessed by a Sperm Class Analyzer (SCA 2002; Microptic, Barcelona, Spain).

Viability assessment of spermatozoa

The proportions of living and dead sperm were assessed by a living-cell nucleic acid stain (SYBR-14), in combination with the conventional dead-cell nucleic acid stain propidium iodide (41), using the staining protocol of a live/dead sperm viability kit (Molecular Probes, Eugene, OR). At least 500 sperm were counted for each treatment.

Sucrose gradient fractionation of membranes

The separation of membrane fractions was performed as previously reported (46) with same modifications. Frozen testis samples from WT and HSL-KO mice were homogenized in 2 ml of 500 mM sodium carbonate (pH 11) and protease inhibitor cocktail (Pierce Biotechnology, Rockford, IL) using a Dounce homogenizer. Then, the homogenates were centrifuged for

30 min at $14,000\ g$ to obtain a Golgi-free supernatant and disrupted by sonication for three bursts of 30 s each. Equal amounts of membrane proteins were then adjusted to 42.5% sucrose prepared in MBS [25 mM Mes (pH 6.5) and 0.15 M NaCl]. A 5–35% discontinuous sucrose gradient was formed above, and the tube was centrifuged at $190,000\ g$ for 18–20 h in a SW41 rotor (Beckman Instruments, Palo Alto, CA). Twelve 1 ml fractions were collected from the top of the gradient and processed for caveolin-1 (Cav-1) (Santa Cruz Biotechnology, Santa Cruz, CA) and anti-transferrin receptor (TfR; Zymed, Invitrogen, San Francisco, CA) analysis by Western blotting. The fractions were concentrated with 10% trichloroacetic acid precipitation prior to electrophoretic analysis for SR-BI and SR-BII (Novus Biologicals, Littleton, CO) by Western blotting. The sample proteins were measured using a bicinchoninic acid (BCA) protein assay (Pierce Biotechnology).

Western blotting

Western blot analysis was performed as previously described (35). The samples were homogenized in 10 mM Tris-HCl buffer (pH 7.4) containing 1 mM EDTA, 12 mM 2-mercaptoethanol, 1 mM benzimidazole, and 1 mM phenylmethylsulphonyl fluoride, with the addition of a cocktail of protease inhibitors (10 $\mu\text{g}/\text{ml}$ of leupeptin and 1 $\mu\text{g}/\text{ml}$ of aprotinin) and phosphatase inhibitors (10 mM sodium fluoride and 1 mM sodium orthovanadate) in the presence of 0.5% Triton X-100. An equal amount of protein from each gradient fraction or whole-cell lysate (20–50 μg) were subjected to 8–12% SDS-PAGE and transferred to polyvinylidene difluoride (PVDF) or nitrocellulose membranes (GE Millipore, Bedford, MA). After blocking, the blots were probed with specific antibodies followed by incubation with horseradish peroxidase-conjugated secondary antibodies (Santa Cruz Biotechnology). The immunoblots were incubated with the enhanced chemiluminescence reagent (Bio-Rad) and exposed to X-ray film or for equal times on a VersaDoc MP 4000 System (Bio-Rad) and images were obtained. The density of the bands was quantified by using the Quantity One 4.5.2 version program (Bio-Rad). The specificity of the procedure was assessed by means of negative controls that were performed omitting the primary antibody and incubating only with the secondary antibody at optimal titers. Phospho-Akt-S473, Akt, phospho-p38, and p38 antibodies were obtained from Cell Signaling Biotechnology (Danvers, MA), diphospho-ERK1/2 and ERK1/2 (Sigma-Aldrich, St. Louis, MO), phospho-SRC (BD Biosciences, San Jose, CA), caveolin-1 and GADPH (Santa Cruz Biotechnology), SR-BI and SR-BII (Novus Biologicals, Littleton, CO), HSL (Chemicon, Billerica, MA), and TfR (Zymed, Invitrogen).

Immunohistochemistry

Streptavidin-peroxidase immunostaining was performed, as previously described (28, 35). Briefly, the sections were incubated for 12 h at 4°C with the primary antibody [anti-SR-BI and SR-BII (1/1000), anti-LIMP II (1/700), and anti-HSL 1:800; chicken polyclonal antiserum directed against HSL from white rat adipose tissue diluted in 0.3% normal goat serum, 0.001% Triton X-100, and 0.01% glycine in TBS (pH 7.6)]. The sections were washed twice in TBS to remove unbound primary antibody, then incubated with the secondary antibody for 1 h at room temperature. The secondary biotin-conjugated antibodies were anti-rabbit IgG (1/500) for SR-BI and SR-BII (Novus Biologicals, Littleton, CO), anti-goat IgG (1/400) for LIMP II (R and D Systems, Minneapolis, MN), and goat anti-chicken IgY (1:200) for HSL (Vector Labs, Burlingame, CA), diluted in 0.3% normal rabbit or goat serum, 0.001% Triton X-100, and 0.01% glycine in TBS. Sections were rinsed in TBS and incubated with the streptavidin-peroxidase complex (Zymed Labs, San Francisco CA) for 30 min, and washed

in TBS followed by Tris-HCl buffer (pH 7.6). Peroxidase activity was developed using 3,3'-diaminobenzidine tetrahydrochloride (DAB) as the chromogen (Sigma-Aldrich). The sections were counterstained with Carazzi's hematoxylin. Thereafter, the sections were dehydrated in ethanol, cleared with xylene, mounted in DePeX, and observed under a light microscope.

The specificity of the immunohistochemical procedures was assessed by means of negative controls that were performed as follows: omitting the primary antibodies; using nonimmune serum instead of the primary antibodies; and incubating with an inappropriate secondary antibody after the incubation with the primary antibodies at optimal titers.

The staining intensity was qualitatively evaluated and classified as absent (-), weak (+), moderate (++), or intense (+++). The assessment of the grade of staining was performed in a blinded way by two independent investigators under a high-power field ($\times 400$) using standard light microscopy. When there was a disagreement between observers on scores, the observers were blinded to the last score and consensus judgement was reached through discussion.

Neutral lipid staining with Oil Red O

Tissue sections were immersed in isopropanol for 3–5 s and incubated in a solution of 5 g Oil Red O/100 ml of isopropanol diluted 2/3 in H₂O for 20–30 min in dark at room temperature. Subsequently, the sections of tissues were washed with isopropyl alcohol, then with water. The sections were contrasted with Carazzi's hematoxylin (Panreac) and embedded for 10 min, washed with distilled water, and mounted in aqueous medium (glycerol/PBS). The slides were visualized on a confocal microscope (Nikon C1 Eclipse Ti-e, Japan).

Free cholesterol staining with filipin

Tissue sections were incubated in a solution of filipin (Sigma-Aldrich) (0.1 $\mu\text{g}/\mu\text{l}$) during 1 h in dark at room temperature. Subsequently, the sections of tissues were washed three times with PBS and mounted in NonFade medium (Invitrogen). The slides were visualized on a confocal microscope (Nikon C1 Eclipse Ti-e, Japan).

RNA isolation and real-time quantitative RT-PCR

Total RNA from testis was extracted using TriReagent (Sigma) and reverse transcribed using M-MLV reverse transcriptase enzyme (Promega, WI) in the presence of the RNase inhibitor RNasin (2 U/ μl) (Promega). Real-time quantitative PCR (qRT-PCR) amplification was performed on a LightCycler 480 using the SYBR Green I Master kit (Roche Applied Science). The thermocycle protocol was 95°C for 5 min, followed by 45 cycles of 95°C for 10 s, 60°C for 10 s, and 72°C for 10 s. We evaluated the melting curves for each gene and separated the PCR reaction products on 2% agarose gels to confirm the presence of a single product. We analyzed the efficiency of the reaction by amplifying serial dilutions of cDNA (1:10, 1:100, 1:1000, and 1:10000). We ensured that the relationship between the threshold cycle (Ct) and the log (RNA) was linear ($-3.6 < \text{slope} < 3.2$). All analyses were performed in triplicate, and the target gene copy number was normalized against the housekeeping gene CypB (encoding cyclophilin B). The primers used in the real-time PCR are shown in supplementary Table I.

Statistical analysis

Data are presented as the mean \pm SEM unless otherwise stated. All statistical analyses were performed with Graph Pad Prism, version 4 (GraphPad Software, San Diego, CA). For comparison between WT and KO animals, two-way ANOVA was conducted and

the significance of difference was assessed using a paired Student *t*-test. Data were considered significant at a $P < 0.05$ ($*P < 0.05$, $**P < 0.01$, and $***P < 0.001$).

RESULTS

Body weight and plasma levels of lipids and testosterone in wild-type (HSL^{+/+}) and HSL KO (HSL^{-/-}) mice

HSL is a lipolytic enzyme, and the lack of this protein could affect body weight. We observed that body weight was significantly reduced (27%) in adult HSL^{-/-} mice compared with HSL^{+/+} mice (Fig. 1A). No differences in plasma testosterone concentration between the two groups of animals were found (Fig. 1B). Plasma total cholesterol levels were significantly higher in HSL^{-/-} mice than in controls, whereas the triglyceride concentration did not differ between groups (Fig. 1C).

Testis weight, number of spermatozoa, motility per epididymidis, and histological study in wild-type (HSL^{+/+}) and HSL-KO (HSL^{-/-}) mice at 16 weeks of age

The testis weight was reduced in HSL^{-/-} mice compared with HSL^{+/+} mice (Fig. 2A). HSL^{-/-} mice are sterile, and we sought to know whether the reduction in the testis weight of the HSL^{-/-} mice has an effect in the number and motility of the spermatozoa. Sperm counts in epididymis preparations revealed that the number of spermatozoa per epididymis in HSL^{-/-} mice was 1.5 ± 1.8 spermatozoa/ml and $16.6 \pm 1.2 \times 10^6$ spermatozoa/ml in HSL^{+/+} mice. HSL^{-/-} spermatozoa in the epididymis were not motile and were dead, whereas 50% of the spermatozoa from HSL^{+/+} mice were motile and 60% were alive (Fig. 2A). In summary, HSL^{-/-} mouse testes have a very low number of spermatozoa, and the spermatozoa were not motile.

Testis histology after hematoxylin/eosin staining showed that adult HSL^{-/-} mouse testis (16 weeks) were atrophic (Fig. 2B). Semi-thin cross-sections of testes revealed a 40% decrease in the average diameter of seminiferous tubules (ST), exhibiting reduction and disorganization of the multilayered seminiferous epithelium. The thickness of the epithelial layer of the HSL^{-/-} seminiferous tubules was greatly reduced, from 12 to 5–7 layers. Together with the complete absence of mature spermatozoa, the number of mature spermatids was also markedly reduced. Extensive vacuolation was observed in the epithelial cells. The vacuoles may contain CE because it has been described that CE content is increased 2.3-fold in HSL^{-/-} mice (4). The intertubular space of the HSL^{-/-} testis was occupied by proliferating Leydig cells (LC) in clusters of all developmental stages (Fig. 2B). We observed an increased number of LCs in HSL^{-/-} testis mice compared with HSL^{+/+} mice. In HSL^{+/+}, the lamina propria of the ST is composed of a continuous layer of flat elongated myoid cells (MC) separated by a rather thin basal lamina from ST and the endothelium of lymphatic capillaries. In HSL^{-/-} mouse testis, the lamina propria increases in thickness and proliferation of myoid cells correlates with thickening of basement membranes.

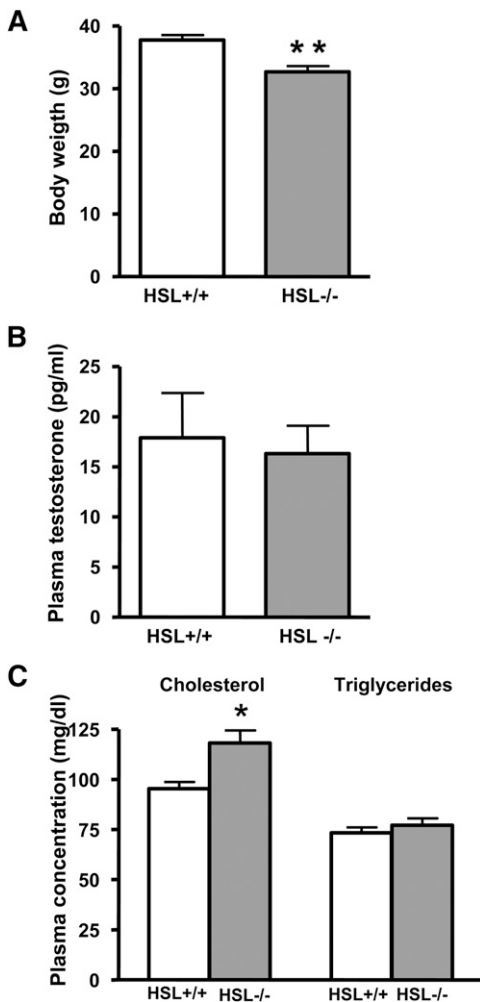


Fig. 1. Effects of HSL deficiency on the body weight (A), plasma testosterone (B), and plasma total cholesterol and triglycerides (C) in wild-type (HSL^{+/+}; open bar) and HSL knockout (HSL^{-/-}; solid bar) mice. Mice used in these experiments were 16 weeks old. Data are expressed as the means \pm SEM of 8 mice per experimental group. Statistical comparisons are shown versus HSL^{+/+} by Student *t*-test (**P* < 0.05, ***P* < 0.01).

HSL localization and protein expression in wild-type (HSL^{+/+}) and HSL KO (HSL^{-/-}) mouse testis

First, we decided to study the distribution of HSL in the testis of HSL^{+/+} mice and confirm its absence in HSL^{-/-} mice by immunohistochemistry (supplementary Fig. 1). No staining was noted in any of the negative controls (data not shown). HSL^{+/+} mouse testis showed HSL-positive staining in the cytoplasm of the Leydig cells and in the elongated spermatids of the ST. However, as expected, HSL^{-/-} mouse testis was immunonegative for HSL.

We then analyzed the protein expression by Western blotting in total lysates of mouse testes. HSL^{+/+} mouse testis showed the main immunoreactive HSL protein to be 130 kDa in this tissue (supplementary Fig. 1). HSL^{-/-} mouse testis showed no immunoreactive HSL protein (supplementary Fig. 1).

We then studied the expression and cellular localization of key proteins in lipid metabolism of the testis and the histologic analysis of neutral lipids in the testis to determine

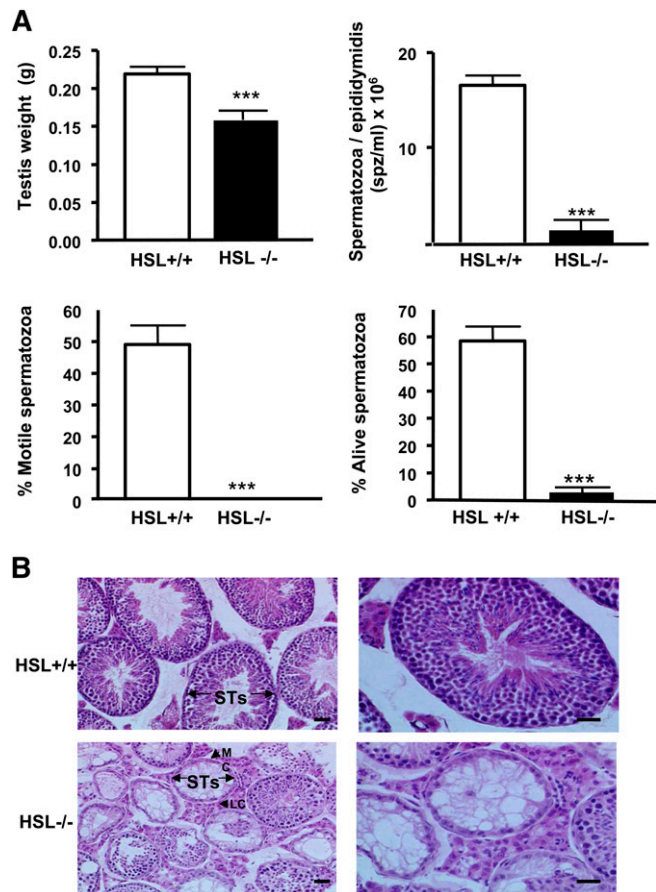


Fig. 2. Effects of HSL deficiency on the testis weight, number of spermatozoa and motility per epididymis (A) and histology of testis stained with hematoxylin/eosin (B), in wild-type (HSL^{+/+}) and HSL knockout (HSL^{-/-}) mice at 16 weeks of age. The diameter of seminiferous tubules (ST), the localization of Leydig cells (LC), and flat elongated myoid cells (MC) are indicated by arrows. Mice used in these experiments were 16 weeks old. Data are expressed as the means \pm SEM of 8 mice per experimental group. Statistical comparisons are shown versus HSL^{+/+} by Student *t*-test (****P* < 0.001). (B) Bars = 25 μ m and 50 μ m.

whether the location or quantity was affected by the lack of HSL.

Free-cholesterol staining with filipin and neutral-lipids staining with Oil Red O of wild-type (HSL^{+/+}) and HSL KO (HSL^{-/-}) mouse testis

We observed positive staining of free cholesterol with filipin (Fig. 3A) and neutral lipids with Oil Red O (Fig. 3B) in the Leydig cells from HSL^{+/+} and HSL^{-/-} mouse testes, seemingly more abundant in the testes that lack HSL, which indicates an accumulation of neutral lipids in the Leydig cells of mice lacking the HSL compared with controls.

Class B scavenger receptor (SR-BI, SR-BII, and LIMP II) localization and protein and mRNA expression in wild-type (HSL^{+/+}) and HSL KO (HSL^{-/-}) mouse testis

We analyzed the expression of the different SR-B in testis due to their relevance for cholesterol utilization for steroidogenesis and spermatogenesis. With respect to SR-BI, in HSL^{+/+} mice, positive staining was found in the membranes

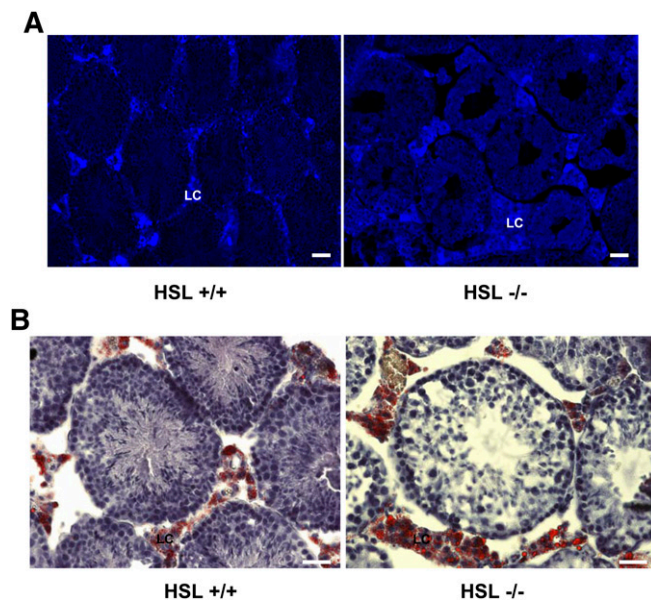


Fig. 3. Free cholesterol staining with filipin (A) and neutral lipid staining with Oil Red O (B) of wild-type (HSL^{+/+}) and HSL knockout (HSL^{-/-}) mice testes showing positive staining in Leydig cells (LC). The figures show the results of one representative immunohistochemistry of eight experiments per group. (A) Bars = 25 μ m. (B) Bars = 50 μ m.

of the Leydig cells and in some spermatids. HSL^{-/-} testis shows a great increase in SR-BI-positive staining in the Leydig cells (Fig. 4A). To confirm these results, SR-BI protein levels were determined by Western blotting. HSL^{+/+} testis expressed two SR-BI immunoreactive proteins. The apparent molecular masses of the immunoreactive bands were 82 kDa (mature protein, intense band) and 57 kDa (immature protein, light band). HSL^{-/-} testis showed an increased intensity of these two SR-BI proteins compared with HSL^{+/+} mouse testis (Fig. 4A).

The results of SR-BII localization and protein expression in HSL-WT (HSL^{+/+}) and HSL-KO (HSL^{-/-}) mouse testis are shown in Fig. 4B. HSL^{+/+} mouse testis showed SR-BII-positive staining in the membrane of the germinal cells (spermatocytes and round spermatids) and negative staining in elongated spermatids, and in Sertoli and Leydig cells. HSL^{-/-} testis showed increased SR-BII-positive staining in the membranes of the germinal cells from the ST. By Western blotting, an increase in the expression of SR-BII (82 kDa) was observed in HSL^{-/-} mouse testis (Fig. 4B).

LIMP-II staining was positive in the membrane of the Sertoli cells and slightly more in Leydig cells from HSL^{+/+} mouse testis (Fig. 4C). HSL^{-/-} testis showed increased LIMP-II-positive staining in Sertoli and Leydig cells compared with HSL^{+/+} mouse testis (Fig. 4C).

Finally, we measured the SR-B mRNA levels. SR-BII and LIMP-II mRNA expression was significantly increased in HSL^{-/-} mouse testis compared with HSL^{+/+} mouse testis (Fig. 4D). No changes were observed in SR-BI mRNA levels among the studied groups.

Taken together, these results indicate a specific cell-type localization of the SR-B in mouse testis. Thus, in HSL^{+/+}

mouse testis, SR-BI was localized to the surfaces of Leydig and spermatid cells. SR-BII was localized to the membranes of germinal cells (spermatocytes and spermatids) from the ST, Leydig and Sertoli cells were immunonegative for SR-BII. LIMP II was mainly localized in the membranes of the Sertoli cells and less so in Leydig cells. The lack of HSL in mouse testis induces an increased SR-B expression that could contribute to increase CE uptake from the plasma lipoproteins by these receptors.

Class B scavenger receptor distribution onto lipid raft and nonraft plasma membrane microdomains and signaling cascades activation in wild-type (HSL^{+/+}) and HSL-KO (HSL^{-/-}) mouse testis

To determine whether the decreased availability of free cholesterol in HSL-KO (HSL^{-/-}) mouse testis could compromise the amount of cholesterol in the plasma membrane and, specifically, the formation and functionality of the lipid raft structures, we isolated plasma membrane fractions from mouse testis in a sucrose density gradient analyzing protein expression by Western blot. In HSL^{+/+} mouse testis, immunoreactive caveolin-1 was mainly detected in fractions 2 and 3, indicating that these fractions contain lipid rafts, whereas TfR, a marker of the nonraft membrane domain, was only detected in fractions 8–11 (Fig. 5A). The lack of HSL in mouse testis resulted in a significant decrease in caveolin-1 content in lipid raft fractions, whereas there was an increase in caveolin-1 in nonraft fractions compared with the control (Fig. 5A). Thus, HSL led to a shift in the distribution of caveolin-1 from lipid rafts to denser membrane domains.

We then studied whether the lipid raft disruption affected or altered SR-B (SR-BI and SR-BII) plasma membrane localization and expression. In the testes of the control (HSL^{+/+}) and HSL^{-/-} mice, the mature form of SR-BI (82 kDa) was present in both plasma membrane domains (lipid raft and nonraft; Fig. 5B). In contrast, the immature form of SR-BI (57 kDa) was localized only in nonraft plasma membrane fractions. No differences in the localization of both forms in the plasma membrane fractions between the two groups of animals were found (Fig. 5B). In HSL^{-/-} mice, we observed an increase in the expression of the mature and immature forms of the SR-BI receptor in both microdomains compared with controls (Fig. 5B).

SR-BII was present in both plasma membrane domains (Fig. 5C), and there were no differences in the distribution or expression in the testes of HSL^{-/-} mice compared with controls.

It has been reported that the binding of HDL to SR-BI activates the signaling cascades of the SRC family kinases [phosphatidylinositol 3-kinase (PI3K)/AKT and MAPK] in endothelial cells (47). Thus, we next sought to determine whether these signaling pathways were affected by the lack of HSL. The testes of HSL^{+/+} mice expressed total and phosphorylated forms of the proteins ERK1/2, AKT, and Fyn (SRC) (Fig. 6). There was an increase in the expression of p-ERK, p-AKT, and p-SRC in HSL^{-/-} mouse testis lysates versus HSL^{+/+} mouse testis, without any change in the total form of the proteins studied (Fig. 6).

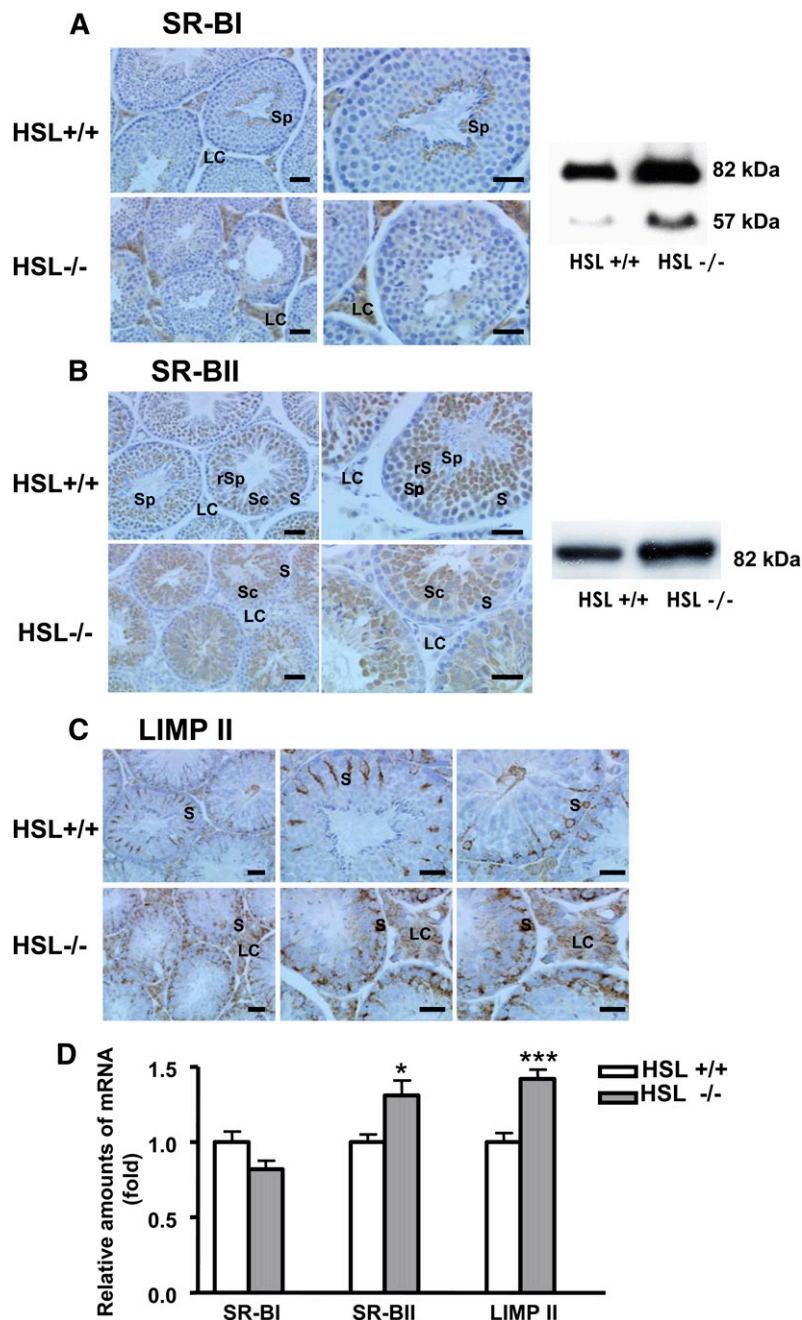


Fig. 4. Effects of the lack of HSL in the immunolocalization, expression of SR-BI (A), SR-BII (B), and LIMP II (C) proteins and mRNA of class B scavenger receptors (SR-BI, SR-BII, and LIMP II) (D) in wild-type (HSL^{+/+}) and HSL knockout (HSL^{-/-}) mice testis. Testis were removed from mice, embedded in paraffin, sectioned, incubated with the primary antibodies, and counterstained with Carazzi's hematoxylin. A: Immunohistochemistry with SR-BI antibody followed by a secondary antibody conjugated with biotin shows positive staining in the cytoplasm of Leydig cells (LC) and elongated spermatids (Sp) of the seminiferous tubules of HSL^{+/+} mice testis. Western blotting analysis of SR-BI protein in mice testis shows the expression of the 82 kDa (mature isoform) and 57 kDa (immature isoform) of SR-BI receptor. B: Immunohistochemistry for SR-BII shows positive staining in the membrane of the germinal cells [spermatocytes (Sc) and round spermatids (rS)] and negative staining in elongated spermatids (Sp), Sertoli cells (S), and Leydig cells (LC). Western blotting reveals an increased expression of SR-BII (82 kDa) in HSL^{-/-} mice testis. C: Immunohistochemistry with LIMP II shows positive staining in the membrane of the Sertoli cells (S) and Leydig cells (LC). D: mRNA expression of class B scavenger receptors (SR-BI, SR-BII, and LIMP II) as measured by qRT-PCR. mRNA levels were normalized to CypB mRNA. Data show mean \pm SEM of 5–7 animals relative to WT mice. * $P < 0.05$; *** $P < 0.0005$. Mice used in these experiments were 16 weeks old. The figures show the results of one representative immunohistochemistry of eight individual experiments per group (A, B, and C). Bars: 25 μ m and 50 μ m.

These results show that HSL^{-/-} mouse testis has increased expression of the SR-BI mature isoform in plasma membrane lipid raft fractions and increased expression of the SR-BI immature isoform in the plasma membrane nonraft fractions with respect to the HSL^{+/+} mouse testis. This could be associated with the activation of different signaling pathways (AKT, ERK, and SRC) mediated by the SR-B.

DISCUSSION

The absence of HSL in testes results in severe oligospermia and infertility, underscoring the importance of this enzyme in spermatogenesis (4, 36). The lack of HSL disturbs tissue lipid composition and cholesterol metabolism

(4, 36). The absence of CEH activity in HSL^{-/-} mouse testis may induce a decrease in the hydrolysis of CE that causes a reduction in the availability of free cholesterol, which is involved in cell proliferation (48, 49) and, therefore, in spermatogenesis. The aim of the present work was to study the SR-B cellular expression in HSL^{-/-} mouse testis for their potential importance in cholesterol provision, as well as their localization to lipid rafts and the activity of related signaling cascades, which ultimately may be involved in infertility in HSL^{-/-} male mice.

In the present study, we found profound alterations in the morphology of HSL^{-/-} mouse testis, affecting both the intertubular space, with increased number of Leydig and myoid cells, and the seminiferous tube, with disrupted epithelium and reduced number of mature spermatids, all

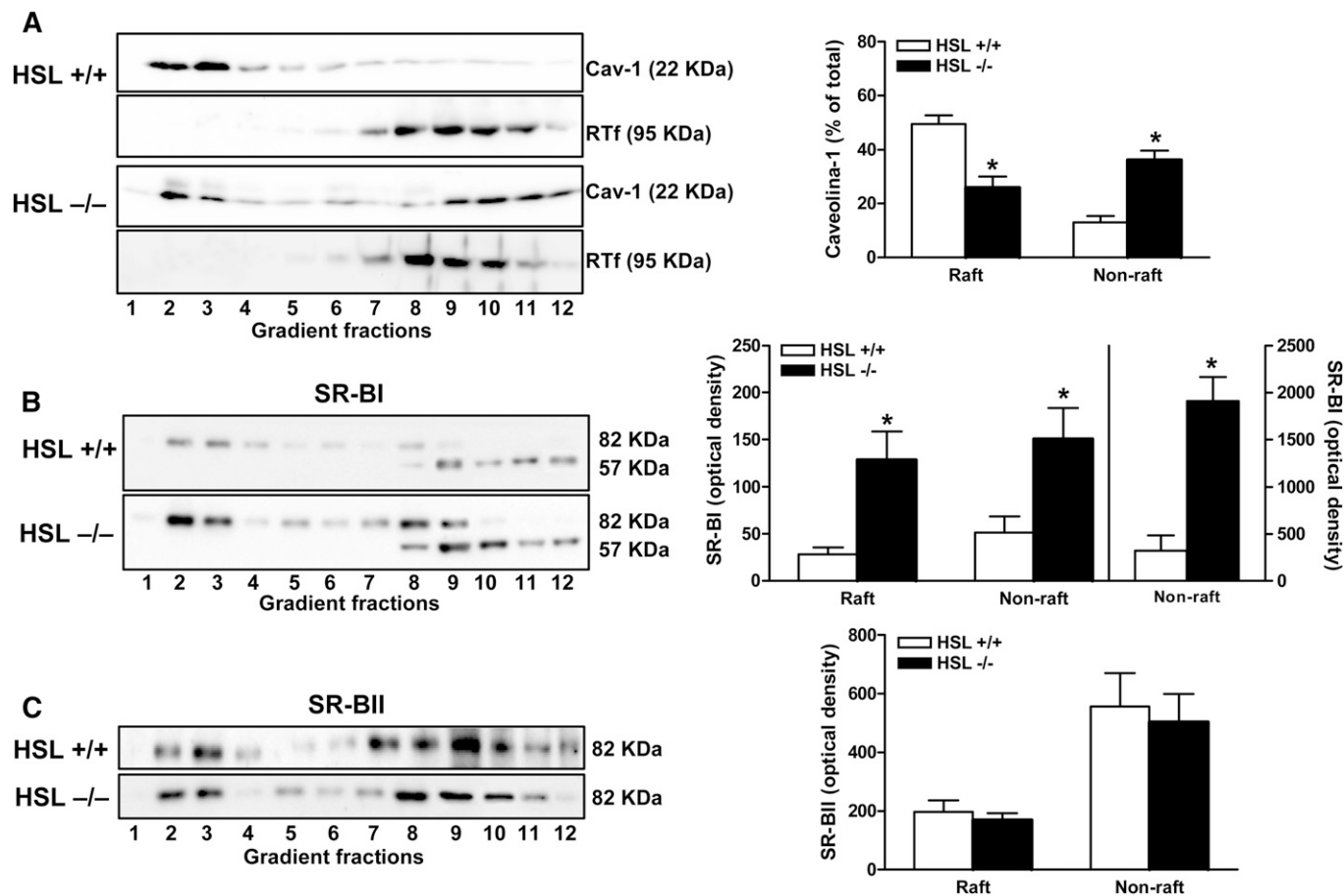


Fig. 5. Effects of HSL deficiency on testis plasma membrane microdomains. (A) Western blotting of gradient fractions from HSL^{+/+} and HSL^{-/-} mice testis with anti-caveolin-1 (Cav-1) and anti-transferrin (anti-TfR) antibodies shows the expression of Cav-1 in lipid raft fractions (fractions 1 and 2) and TfR in nonraft fractions (fractions 8–11). Bars graph shows the densitometric analysis of caveolin-1 Western blots in which caveolin-1 levels are expressed as a percentage of total caveolin-1 (raft, fractions 2+3; nonraft, fractions 8+9+10) (n = 9, mean ± SEM). (B) Western blotting for SR-BI in gradient fractions from HSL^{+/+} and HSL^{-/-} mice testis. Bars graph shows the densitometric analysis of SR-BI individual bands (mature and immature form) Western blots (arbitrary units) (raft, fractions 2+3; nonraft, fractions 8+9+10) (n = 6, mean ± SEM). (C) Western blots for SR-BII in gradient fractions from HSL^{+/+} and HSL^{-/-} mice testis. Bars graph shows the densitometric analysis of SR-BII individual bands Western blots (arbitrary units) (raft, fractions 2+3; nonraft, fractions 8+9+10) (n = 5, mean ± SEM). Representative immunoblots are shown in A, B, and C. Statistical comparisons are shown versus HSL^{+/+} (*P < 0.05).

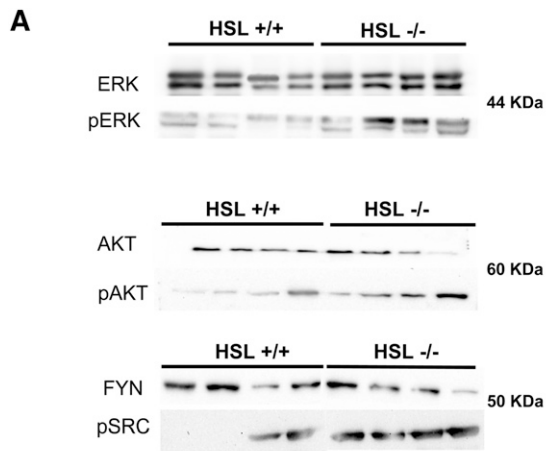
confirming previous results reported by others (4, 36). These morphological changes were accompanied by severe oligospermia, with the decreased sperm count and reduced sperm motility shown by HSL^{-/-} male mice (Refs. 4, 50, 51 and present results). The acquisition of sperm motility and fertility have been associated with changes in cholesterol content of male gametes during the transit through the epididymis (52) and during capacitation (53). Inadequate cholesterol levels in the sperm apparently cause infertility in humans (54).

Testes from HSL^{+/+} mice mainly express the immunoreactive HSL protein of 130 kDa. We found that HSL is located in Leydig cells, which suggests that HSL may be involved in CE hydrolysis to provide free cholesterol for the synthesis of steroid hormones in physiological conditions. However, oligospermia in the HSL^{-/-} male mouse does not appear to result from hypogonadism. Actually, HSL^{-/-} mice have normal plasma levels of follicle-stimulating hormone, luteinizing hormone (4, 51), and testosterone (Refs. 4, 51 and present results). Other sources

of free cholesterol for steroidogenesis may be operating in the HSL^{-/-} mouse, including the endogenous cholesterol biosynthesis and the hydrolysis of lipoprotein-derived CE within the lysosomes.

The lack of HSL resulted in the augmented deposit of lipid droplets observed in Leydig cells, confirming the inability of HSL-lacking cells to utilize esterified lipids. This observation is in accordance with previous results by others showing the accumulation of both CE (4) and DAG (51) in the HSL^{-/-} testis. The absence of CE hydrolase activity may compromise the availability of free cholesterol, which is required for cell proliferation (48, 49) and, therefore, for spermatogenesis.

In the testis, the main pathway to obtain cholesterol is the selective uptake of CE from HDL mediated by SR-BI (18, 20, 55). The SR-BI receptor also mediates the bidirectional flow of unesterified cholesterol and phospholipids between HDL and cells (56). SR-BII, which is an isoform of the SR-BI gene formed by alternative splicing of the transcript (41), also binds HDL with high affinity, but it



B

	HSL +/+	HSL -/-
ERK	1 272.00 ± 76.50	1551.00 ± 189.00
pERK	9.04 ± 2.47	34.35 ± 2.39*
AKT	20.21 ± 14.37	31.45 ± 16.45
pAKT	3.73 ± 1.767	12.17 ± 1.92*
FYN	46.73 ± 6.97	37.74 ± 11.84
p-SRC	10.98 ± 2.79	31.24 ± 11.14*

Fig. 6. Effects of HSL deficiency on testis MAPK signaling pathways. A: Western blots for ERK, pERK, AKT, pAKT, FYN, and pSRC in HSL^{+/+} and HSL^{-/-} mice testis. Results are shown for one Western blot including four animals per group, representative of 5–6 individual experiments per group. There was an increase in the expression of p-ERK, AKT, p-AKT, and p-SRC in HSL^{-/-} mice testis versus HSL^{+/+} mice testis, without any change in the total forms of the proteins. B: Values were calculated by densitometry of the individual bands of the different proteins, and they represent the means ± SEM of n = 5–6 samples per experimental group. Statistical comparisons are shown versus HSL^{+/+} by Student *t*-test (**P* < 0.05).

differs from SR-BI in that it mediates HDL endocytosis through a clathrin-dependent, caveolae-independent pathway (57) and does not mobilize the intracellular stores of CE (58).

In the present study, in the HSL^{+/+} control mouse testis, we show that SR-BI is located in the membrane of Leydig cells and on elongated spermatids, which agrees with previous studies in other species (57, 59, 60), including humans (35). Unlike other species (35, 60), we could not detect SR-BI in Sertoli cells. Of note, testis of HSL^{-/-} mice showed an increased expression of SR-BI as determined by immunostaining, particularly in Leydig cells. This was confirmed by Western blot, showing a high increase in the protein expression of the two forms of SR-BI, the mature (82 kDa) and the immature (57 kDa) forms, in testis from mice lacking HSL. To further analyze the changes in SR-BI expression, we measured mRNA levels by qRT-PCR. Intriguingly, there were no differences in SR-BI mRNA levels between the two groups. This latter result indicates that the increased SR-BI protein expression observed in HSL^{-/-} mouse testis is not due to increased transcription. Recently, Dong et al.

(61) described that the induction of SR-BI protein expression by both tamoxifen and 4-hydroxytamoxifen was independent of transcription. Actually, these authors demonstrated that SR-BI mRNA levels and promoter activity were not influenced by any of these selective estrogen-receptor modulators; instead, these drugs increased the stability of SR-BI protein (61). It may be speculated that HSL deficiency also increases SR-BI protein stability.

SR-BII is located in the membranes of germinal cells (spermatocytes and spermatids) from the ST (Ref. 60 and present results), whereas Leydig and Sertoli cells were found to be immunonegative for SR-BII. Mice lacking HSL showed an increased expression of SR-BII in testicular cells as observed by immunohistochemistry, which corresponded with augmented SR-BII protein and mRNA levels in the whole tissue. Finally, LIMP II was located in the membranes of Sertoli and Leydig cells, and similar to the other SR-B, testes from HSL^{-/-} mice had increased expression of LIMP II as indicated by the increased staining in both cell types (Sertoli and Leydig cells) as well as by the higher mRNA levels in HSL^{-/-} mice testis compared with the WT.

Taken together, the results show an increased expression of SR-B (SR-BI, SR-BII, and LIMP II) in testes in the HSL^{-/-} mouse, which is likely a response to the inability to obtain free cholesterol from CE due to the lack of HSL. This response certainly might facilitate the entry of HDL-CE into the cells, contributing to the intracellular accumulation of CE rather than to alleviating the cholesterol demands.

One of the fates of cellular cholesterol is the formation of lipid rafts structures. We thus studied the distribution of caveolin-1 and SR-B in membrane fractions of HSL^{-/-} mouse testis. The HSL deficiency in mouse testis resulted in an alteration in lipid raft architecture, as evidenced by the shift of caveolin-1 to denser fractions. It has been reported that the reduction of free cholesterol availability impairs the formation of lipid rafts, leading to a redistribution of caveolin-1 to nonraft fractions (46, 62). Therefore, it is suggested that the lack of HSL results in the impairment of lipid-raft/caveolae formation, likely due to the deficiency of free cholesterol.


We found that SR-BI was distributed onto both raft and nonraft fractions from testis plasma membranes. In other cell types, others reported that SR-BI is associated with caveolae. Thus, in steroidogenic cells, Babitt et al. (40) observed that SR-BI copurified with caveolin-1 as isolated by density gradient fractionation and that SR-BI colocalized with caveolin-1 in punctuate microdomains across the cell surface by immunofluorescence microscopy. Moreover, by studying the fate of radiolabeled HDL in CHO cells expressing SR-BI, Graf et al. (63) showed that HDL-CE rapidly associates with caveolin-1-containing fractions and that it is then translocated to an intracellular compartment, thus suggesting that caveolae are acceptors for HDL-derived CE. In contrast, by electron microscopy in different cell types, Peng et al. (44) concluded that SR-BI is localized primarily in clusters on microvillar extensions of the plasma membrane and that it is nearly absent from caveolae. We did not address the functional site of SR-BI. The coisolation

of the SR-BI mature form (82 kDa) and caveolin-1 in low-density membrane fractions does not necessarily indicate that both proteins are within the same morphological structure in the cell. The possibility exists that SR-BI localizes to lipid rafts not containing caveolin-1. Nevertheless, the fact that the immature form of SR-BI (57 kDa) was excluded from these structures, whether lipid rafts or caveolae, firmly suggests that they are physiologically relevant in the function of SR-BI in the testis. In plasma membranes from HSL^{-/-} mice, the levels of SR-BI, both the mature and the immature forms, were highly increased compared with the WT, which is in accordance with the augmented expression observed in whole tissue; however, the distribution between the raft and nonraft fractions was not altered.

Regarding SR-BII, it was localized in both the lighter and, mostly, in the denser plasma membrane fractions considered, and this distribution was not affected by the HSL status.

Lipid rafts/caveolae not only influence cholesterol homeostasis by acting as conduits for cellular flux (38) but also concentrate signaling proteins for signal transduction (39). It has been reported that HDL binding to SR-BI leads to the activation of a tyrosine kinase (SRC), which causes the activation of PI3K and subsequent activation of AKT and MAPK in endothelial cells (47). We report herein that different signaling pathways (AKT, ERK, and SRC) are activated in the HSL^{-/-} mouse testis. The significance of these results is unknown; however, the activation of MAPK cascades is involved in differentiation, proliferation, and other cellular processes during spermatogenesis (64–67).

The exact mechanism through which HSL deficiency produces male infertility remains elusive. The observed alterations in SR-B expression, lipid raft composition, and signaling cascades, however, may provide some clues. First, infertility of HSL-KO mice is not associated with hypogonadism or adrenal insufficiency, as no changes in plasma testosterone levels in HSL-KO were observed (present results and Ref. 4). On the other hand, the increased expression of SB-BI and SR-BII in HSL^{-/-} testis may favor the uptake of CE from HDL and the activation of cell signaling pathways (ERK, AKT, and SRC) involved in differentiation, proliferation, and other cellular processes during spermatogenesis. In this sense, SR-BI overexpression may be contemplated as an attempt to provide cells with cholesterol. However, due to the lack of HSL, the internalized CE cannot be hydrolyzed, and hence, it accumulates in the cytoplasm, contributing to steatosis. This inadequate supply of free cholesterol could be involved in the observed lipid-raft disruption. Finally, functional cholesterol deficiency may compromise cell division (68), thereby interfering with spermatogenesis. Obviously, this is a speculation that requires further studies in vitro with selected cell types to confirm the proposed mechanisms.

In summary, present results indicate that the lack HSL in HSL^{-/-} mice dramatically disrupts cholesterol homeostasis in the testis, with augmented expression of SR-B (SR-BI, SR-BII, and LIMP II), altered lipid-raft microdomains, and activation of different signaling pathways (p-ERK, p-AKT, and p-SRC) with relevance in spermatogenesis. 

The authors thank Irene Buendía, Milagros Lerma, Paloma Mariscal, Ángela Murua, and Nuria Quesada for excellent technical assistance.

REFERENCES

- Eddy, E. M. 1998. Regulation of gene expression during spermatogenesis. *Semin. Cell Dev. Biol.* **9**: 451–457.
- Hecht, N. B. 1998. Molecular mechanisms of male germ cell differentiation. *Bioessays*. **20**: 555–561.
- Hodgson, Y. M., D. C. Irby, J. B. Kerr, and D. M. de Kretser. 1979. Studies of the structure and function of the Sertoli cell in a seasonally breeding rodent. *Biol. Reprod.* **21**: 1091–1098.
- Osuga, J., S. Ishibashi, T. Oka, H. Yagyu, R. Tozawa, A. Fujimoto, F. Shionoiri, N. Yahagi, F. B. Kraemer, O. Tsutsumi, et al. 2000. Targeted disruption of hormone-sensitive lipase results in male sterility and adipocyte hypertrophy, but not in obesity. *Proc. Natl. Acad. Sci. USA*. **97**: 787–792.
- Pasquali, R., L. Patton, and A. Gambineri. 2007. Obesity and infertility. *Curr. Opin. Endocrinol. Diabetes Obes.* **14**: 482–487.
- Gwynne, J. T., and J. F. Strauss 3rd. 1982. The role of lipoproteins in steroidogenesis and cholesterol metabolism in steroidogenic glands. *Endocr. Rev.* **3**: 299–329.
- Rigotti, A., H. E. Miettinen, and M. Krieger. 2003. The role of the high-density lipoprotein receptor SR-BI in the lipid metabolism of endocrine and other tissues. *Endocr. Rev.* **24**: 357–387.
- Kabbaj, O., S. R. Yoon, C. Holm, J. Rose, M. L. Vitale, and R. M. Pelletier. 2003. Relationship of the hormone-sensitive lipase-mediated modulation of cholesterol metabolism in individual compartments of the testis to serum pituitary hormone and testosterone concentrations in a seasonal breeder, the mink (*Mustela vison*). *Biol. Reprod.* **68**: 722–734.
- Wechsler, A., A. Brafman, M. Shafir, M. Heverin, H. Gottlieb, G. Damari, S. Gozlan-Kelner, I. Spivak, O. Moshkin, E. Fridman, et al. 2003. Generation of viable cholesterol-free mice. *Science*. **302**: 2087.
- Rozman, D., M. Seliskar, M. Cotman, and M. Fink. 2005. Pre-cholesterol precursors in gametogenesis. *Mol. Cell. Endocrinol.* **234**: 47–56.
- Bartke, A. 1971. Concentration of free and esterified cholesterol in the testes of immature and adult mice. *J. Reprod. Fertil.* **25**: 153–156.
- Wiebe, J. P., and K. S. Tilbe. 1979. De novo synthesis of steroids (from acetate) by isolated rat Sertoli cells. *Biochem. Biophys. Res. Commun.* **89**: 1107–1113.
- Fofana, M., C. Travert, S. Carreau, and D. Le Goff. 2000. Evaluation of cholesteryl ester transfer in the seminiferous tubule cells of immature rats in vivo and in vitro. *J. Reprod. Fertil.* **118**: 79–83.
- Landschulz, K. T., R. K. Pathak, A. Rigotti, M. Krieger, and H. H. Hobbs. 1996. Regulation of scavenger receptor, class B, type I, a high density lipoprotein receptor, in liver and steroidogenic tissues of the rat. *J. Clin. Invest.* **98**: 984–995.
- Rigotti, A., E. R. Edelman, P. Seifert, S. N. Iqbal, R. B. DeMattos, R. E. Temel, M. Krieger, and D. L. Williams. 1996. Regulation by adrenocorticotrophic hormone of the in vivo expression of scavenger receptor class B type I (SR-BI), a high density lipoprotein receptor, in steroidogenic cells of the murine adrenal gland. *J. Biol. Chem.* **271**: 33545–33549.
- Azhar, S., A. Nomoto, S. Leers-Sucheta, and E. Reaven. 1998. Simultaneous induction of an HDL receptor protein (SR-BI) and the selective uptake of HDL-cholesteryl esters in a physiologically relevant steroidogenic cell model. *J. Lipid Res.* **39**: 1616–1628.
- Temel, R. E., B. Trigatti, R. B. DeMattos, S. Azhar, M. Krieger, and D. L. Williams. 1997. Scavenger receptor class B, type I (SR-BI) is the major route for the delivery of high density lipoprotein cholesterol to the steroidogenic pathway in cultured mouse adrenocortical cells. *Proc. Natl. Acad. Sci. USA*. **94**: 13600–13605.
- Rigotti, A., B. L. Trigatti, M. Penman, H. Rayburn, J. Herz, and M. Krieger. 1997. A targeted mutation in the murine gene encoding the high density lipoprotein (HDL) receptor scavenger receptor class B type I reveals its key role in HDL metabolism. *Proc. Natl. Acad. Sci. USA*. **94**: 12610–12615.
- Imachi, H., K. Murao, M. Sato, H. Hosokawa, T. Ishida, and J. Takahara. 1999. CD36 LIMP II analogous-1, a human homolog of the rodent scavenger receptor B1, provides the cholesterol ester for steroidogenesis in adrenocortical cells. *Metabolism*. **48**: 627–630.

20. Azhar, S., and E. Reaven. 2002. Scavenger receptor class BI and selective cholesteryl ester uptake: partners in the regulation of steroidogenesis. *Mol. Cell. Endocrinol.* **195**: 1–26.
21. Shiratsuchi, A., Y. Kawasaki, M. Ikemoto, H. Arai, and Y. Nakanishi. 1999. Role of class B scavenger receptor type I in phagocytosis of apoptotic rat spermatogenic cells by Sertoli cells. *J. Biol. Chem.* **274**: 5901–5908.
22. Trigatti, B., H. Rayburn, M. Vinals, A. Braun, H. Miettinen, M. Penman, M. Hertz, M. Schrenzel, L. Amigo, A. Rigotti, et al. 1999. Influence of the high density lipoprotein receptor SR-BI on reproductive and cardiovascular pathophysiology. *Proc. Natl. Acad. Sci. USA.* **96**: 9322–9327.
23. Kraemer, F. B., and W. J. Shen. 2002. Hormone-sensitive lipase: control of intracellular tri-(di-)acylglycerol and cholesteryl ester hydrolysis. *J. Lipid Res.* **43**: 1585–1594.
24. Cook, K. G., S. J. Yeaman, P. Stralfors, G. Fredrikson, and P. Belfrage. 1982. Direct evidence that cholesterol ester hydrolase from adrenal cortex is the same enzyme as hormone-sensitive lipase from adipose tissue. *Eur. J. Biochem.* **125**: 245–249.
25. Holm, C., P. Belfrage, and G. Fredrikson. 1987. Immunological evidence for the presence of hormone-sensitive lipase in rat tissues other than adipose tissue. *Biochem. Biophys. Res. Commun.* **148**: 99–105.
26. Kraemer, F. B., S. Patel, M. S. Saedi, and C. Sztalryd. 1993. Detection of hormone-sensitive lipase in various tissues. I. Expression of an HSL/bacterial fusion protein and generation of anti-HSL antibodies. *J. Lipid Res.* **34**: 663–671.
27. Holst, L. S., A. M. Hoffmann, H. Mulder, F. Sundler, C. Holm, A. Bergh, and G. Fredrikson. 1994. Localization of hormone-sensitive lipase to rat Sertoli cells and its expression in developing and degenerating testes. *FEBS Lett.* **355**: 125–130.
28. Martín-Hidalgo, A., L. Huerta, N. Alvarez, G. Alegria, M. Del Val Toledo, and E. Herrera. 2005. Expression, activity, and localization of hormone-sensitive lipase in rat mammary gland during pregnancy and lactation. *J. Lipid Res.* **46**: 658–668.
29. Lobo, M. V., L. Huerta, M. I. Arenas, R. Busto, M. A. Lasuncion, and A. Martín-Hidalgo. 2009. Hormone-sensitive lipase expression and IHC localization in the rat ovary, oviduct, and uterus. *J. Histochem. Cytochem.* **57**: 51–60.
30. Kraemer, F. B., W. J. Shen, K. Harada, S. Patel, J. Osuga, S. Ishibashi, and S. Azhar. 2004. Hormone-sensitive lipase is required for high-density lipoprotein cholesteryl ester-supported adrenal steroidogenesis. *Mol. Endocrinol.* **18**: 549–557.
31. Shen, W. J., S. Patel, V. Natu, R. Hong, J. Wang, S. Azhar, and F. B. Kraemer. 2003. Interaction of hormone-sensitive lipase with steroidogenic acute regulatory protein: facilitation of cholesterol transfer in adrenal. *J. Biol. Chem.* **278**: 43870–43876.
32. Mairal, A., N. Melaine, H. Laurell, J. Grober, L. S. Holst, T. Guillaudoux, C. Holm, B. Jegou, and D. Langin. 2002. Characterization of a novel testicular form of human hormone-sensitive lipase. *Biochem. Biophys. Res. Commun.* **291**: 286–290.
33. Kabbaj, O., C. Holm, M. L. Vitale, and R. M. Pelletier. 2001. Expression, activity, and subcellular localization of testicular hormone-sensitive lipase during postnatal development in the guinea pig. *Biol. Reprod.* **65**: 601–612.
34. Holst, L. S., D. Langin, H. Mulder, H. Laurell, J. Grober, A. Bergh, H. W. Mohrenweiser, G. Edgren, and C. Holm. 1996. Molecular cloning, genomic organization, and expression of a testicular isoform of hormone-sensitive lipase. *Genomics.* **35**: 441–447.
35. Arenas, M. I., M. V. Lobo, E. Caso, L. Huerta, R. Paniagua, and M. A. Martín-Hidalgo. 2004. Normal and pathological human testes express hormone-sensitive lipase and the lipid receptors CLA-I/SR-BI and CD36. *Hum. Pathol.* **35**: 34–42.
36. Chung, S., S. P. Wang, L. Pan, G. Mitchell, J. Trasler, and L. Hermo. 2001. Infertility and testicular defects in hormone-sensitive lipase-deficient mice. *Endocrinology.* **142**: 4272–4281.
37. Vallet-Erdtmann, V., G. Tavernier, J. A. Contreras, A. Mairal, C. Rieu, A. M. Touzalin, C. Holm, B. Jegou, and D. Langin. 2004. The testicular form of hormone-sensitive lipase HSLtes confers rescue of male infertility in HSL-deficient mice. *J. Biol. Chem.* **279**: 42875–42880.
38. Fielding, C. J., and P. E. Fielding. 2000. Cholesterol and caveolae: structural and functional relationships. *Biochim. Biophys. Acta.* **1529**: 210–222.
39. Fielding, C. J., and P. E. Fielding. 2004. Membrane cholesterol and the regulation of signal transduction. *Biochem. Soc. Trans.* **32**: 65–69.
40. Babbitt, J., B. Trigatti, A. Rigotti, E. J. Smart, R. G. Anderson, S. Xu, and M. Krieger. 1997. Murine SR-BI, a high density lipoprotein receptor that mediates selective lipid uptake, is N-glycosylated and fatty acylated and colocalizes with plasma membrane caveolae. *J. Biol. Chem.* **272**: 13242–13249.
41. Webb, N. R., P. M. Connell, G. A. Graf, E. J. Smart, W. J. de Villiers, F. C. de Beer, and D. R. van der Westhuyzen. 1998. SR-BII, an isoform of the scavenger receptor BI containing an alternate cytoplasmic tail, mediates lipid transfer between high density lipoprotein and cells. *J. Biol. Chem.* **273**: 15241–15248.
42. Grewal, T., I. de Diego, M. F. Kirchhoff, F. Tebar, J. Heeren, F. Rinninger, and C. Enrich. 2003. High density lipoprotein-induced signaling of the MAPK pathway involves scavenger receptor type BI-mediated activation of Ras. *J. Biol. Chem.* **278**: 16478–16481.
43. Baranova, I. N., T. G. Vishnyakova, A. V. Bocharov, R. Kurlander, Z. Chen, M. L. Kimelman, A. T. Remaley, G. Csako, F. Thomas, T. L. Eggerman, et al. 2005. Serum amyloid A binding to CLA-1 (CD36 and LIMPII analogous-1) mediates serum amyloid A protein-induced activation of ERK1/2 and p38 mitogen-activated protein kinases. *J. Biol. Chem.* **280**: 8031–8040.
44. Peng, Y., W. Akmentin, M. A. Connolly, S. Lund-Katz, M. C. Phillips, and D. L. Williams. 2004. Scavenger receptor BI (SR-BI) clustered on microvillar extensions suggests that this plasma membrane domain is a way station for cholesterol trafficking between cells and high-density lipoprotein. *Mol. Biol. Cell.* **15**: 384–396.
45. Hogan, B., R. Beddington, F. Costantini, and E. Lacy. 1994. *Manipulating the Mouse Embryo: A Laboratory Manual*. Cold Spring Harbor Press, Cold Spring Harbor, NY.
46. Sánchez-Wandelmer, J., A. Davalos, G. de la Pena, S. Cano, M. Giera, A. Canfran-Duque, F. Bracher, A. Martín-Hidalgo, C. Fernandez-Hernando, M. A. Lasuncion, et al. 2010. Haloperidol disrupts lipid rafts and impairs insulin signaling in SH-SY5Y cells. *Neuroscience.* **167**: 143–153.
47. Mineo, C., I. S. Yuhanna, M. J. Quon, and P. W. Shaul. 2003. High density lipoprotein-induced endothelial nitric-oxide synthase activation is mediated by Akt and MAP kinases. *J. Biol. Chem.* **278**: 9142–9149.
48. Brown, M. S., and J. L. Goldstein. 1974. Suppression of 3-hydroxy-3-methylglutaryl coenzyme A reductase activity and inhibition of growth of human fibroblasts by 7-ketocholesterol. *J. Biol. Chem.* **249**: 7306–7314.
49. Chen, H. W., A. A. Kandutsch, and C. Waymouth. 1974. Inhibition of cell growth by oxygenated derivatives of cholesterol. *Nature.* **251**: 419–421.
50. Wang, S. P., N. Laurin, J. Himms-Hagen, M. A. Rudnicki, E. Levy, M. F. Robert, L. Pan, L. Oligny, and G. A. Mitchell. 2001. The adipose tissue phenotype of hormone-sensitive lipase deficiency in mice. *Obes. Res.* **9**: 119–128.
51. Haemmerle, G., R. Zimmermann, M. Hayn, C. Theussl, G. Waeg, E. Wagner, W. Sattler, T. M. Magin, E. F. Wagner, and R. Zechner. 2002. Hormone-sensitive lipase deficiency in mice causes diglyceride accumulation in adipose tissue, muscle, and testis. *J. Biol. Chem.* **277**: 4806–4815.
52. Haidl, G., and C. Opper. 1997. Changes in lipids and membrane anisotropy in human spermatozoa during epididymal maturation. *Hum. Reprod.* **12**: 2720–2723.
53. Go, K. J., and D. P. Wolf. 1983. The role of sterols in sperm capacitation. *Adv. Lipid Res.* **20**: 317–330.
54. Sugkarroek, P., M. Kates, A. Leader, and N. Tanphaichitr. 1991. Levels of cholesterol and phospholipids in freshly ejaculated sperm and Percoll-gradient-pelleted sperm from fertile and unexplained infertile men. *Fertil. Steril.* **55**: 820–827.
55. Fofana, M., J. C. Maboundou, J. Bocquet, and D. Le Goff. 1996. Transfer of cholesterol between high density lipoproteins and cultured rat Sertoli cells. *Biochem. Cell Biol.* **74**: 681–686.
56. Saddar, S., C. Mineo, and P. W. Shaul. 2010. Signaling by the high-affinity HDL receptor scavenger receptor B type I. *Arterioscler. Thromb. Vasc. Biol.* **30**: 144–150.
57. Eckhardt, E. R., L. Cai, S. Shetty, Z. Zhao, A. Szanto, N. R. Webb, and D. R. Van der Westhuyzen. 2006. High density lipoprotein endocytosis by scavenger receptor SR-BII is clathrin-dependent and requires a carboxyl-terminal dileucine motif. *J. Biol. Chem.* **281**: 4348–4353.
58. Webb, N. R., W. J. de Villiers, P. M. Connell, F. C. de Beer, and D. R. van der Westhuyzen. 1997. Alternative forms of the scavenger receptor BI (SR-BI). *J. Lipid Res.* **38**: 1490–1495.
59. Reaven, E., L. Zhan, A. Nomoto, S. Leers-Sucheta, and S. Azhar. 2000. Expression and microvillar localization of scavenger receptor class B, type I (SR-BI) and selective cholesteryl ester uptake in Leydig cells from rat testis. *J. Lipid Res.* **41**: 343–356.

60. Akpovi, C. D., S. R. Yoon, M. L. Vitale, and R. M. Pelletier. 2006. The predominance of one of the SR-BI isoforms is associated with increased esterified cholesterol levels not apoptosis in mink testis. *J. Lipid Res.* **47**: 2233–2247.
61. Dong, P., T. Xie, X. Zhou, W. Hu, Y. Chen, Y. Duan, X. Li, and J. Han. 2011. Induction of macrophage scavenger receptor type BI expression by tamoxifen and 4-hydroxytamoxifen. *Atherosclerosis*. **218**: 435–442.
62. Brusselmans, K., L. Timmermans, T. Van de Sande, P. P. Van Veldhoven, G. Guan, I. Shechter, F. Claessens, G. Verhoeven, and J. V. Swinnen. 2007. Squalene synthase, a determinant of Raft-associated cholesterol and modulator of cancer cell proliferation. *J. Biol. Chem.* **282**: 18777–18785.
63. Graf, G. A., P. M. Connell, D. R. van der Westhuyzen, and E. J. Smart. 1999. The class B, type I scavenger receptor promotes the selective uptake of high density lipoprotein cholesterol ethers into caveolae. *J. Biol. Chem.* **274**: 12043–12048.
64. Wong, C. H., and C. Y. Cheng. 2005. Mitogen-activated protein kinases, adherens junction dynamics, and spermatogenesis: a review of recent data. *Dev. Biol.* **286**: 1–15.
65. Almog, T., and Z. Naor. 2008. Mitogen activated protein kinases (MAPKs) as regulators of spermatogenesis and spermatozoa functions. *Mol. Cell. Endocrinol.* **282**: 39–44.
66. Lee, J., M. Kanatsu-Shinohara, K. Inoue, N. Ogonuki, H. Miki, S. Toyokuni, T. Kimura, T. Nakano, A. Ogura, and T. Shinohara. 2007. Akt mediates self-renewal division of mouse spermatogonial stem cells. *Development*. **134**: 1853–1859.
67. Blume-Jensen, P., G. Jiang, R. Hyman, K. F. Lee, S. O’Gorman, and T. Hunter. 2000. Kit/stem cell factor receptor-induced activation of phosphatidylinositol 3’-kinase is essential for male fertility. *Nat. Genet.* **24**: 157–162.
68. Martínez-Botas, J., Y. Suarez, A. J. Ferruelo, D. Gomez-Coronado, and M. A. Lasuncion. 1999. Cholesterol starvation decreases p34(cdc2) kinase activity and arrests the cell cycle at G2. *FASEB J.* **13**: 1359–1370.